ELSEVIER

Polymer 42 (2001) 4261–4269

polymer

www.elsevier.nl/locate/polymer

The structures of poly(di-*n*-alkylsilylenemethylene)s

S.-Y. Park[a,b], L.V. Interrante[c], B.L. Farmer[b,*]

[a]*Department of Materials Science and Engineering, University of Virginia, Charlottesville, VA 22903-2442, USA*
[b]*Air Force Research Laboratory, Materials and Manufacturing Directorate, Wright–Patterson Air Force Base, OH 45433-7750, USA*
[c]*Department of Chemistry, Rensselaer Polytechnic Institute, Troy, NY 12180-3590, USA*

Received 8 February 2000; received in revised form 9 October 2000; accepted 9 October 2000

Abstract

The structure of poly(diethylsilylenemethylene) (PDESM), poly(di-*n*-butylsilylenemethylene) (PDBSM), poly(di-*n*-pentylsilylenemethylene) (PDPeSM) and poly(di-*n*-hexylsilylenemethylene) (PDHSM) have been studied using X-ray and electron diffraction methods. The structure of poly(di-*n*-propylsilylenemethylene) (PDPrSM) has been studied and reported in a separate paper. PDBSM, PDPrSM, PDPeSM and PDHSM all have similar packing with a two dimensional monoclinic *ab*-projection of the unit cell. PDESM with the shortest alkyl side chain, has a nearly orthorhombic unit cell ($\gamma^* = \sim 88°$) containing two chains (four repeat units), one at the corner and the second nearly in the center of the *ab*-projection of the unit cell. The backbone conformation of each of these polysilylenemethylenes (PSMs) is all-*gauche*, giving them a 4_1 helical structure. The length of the alkyl side chains affects the packing without changing the backbone conformation.

Keywords: Electron diffraction; Poly(di-*n*-alkylsilylenemethylene)s; Conformation

1. Introduction

Polysilylenemethylenes (PSMs, $[\mathrm{SiRR'CH_2}]_n$) have attracted increasing attention as precursors to silicon carbide fibers [1–3]. Among the potential advantages that this class of polymers may have (as compared to other classes of inorganic/organic hybrid polymers) are a combination of low T_g, high synthetic versatility similar to that of such inorganic backbone polymers as the polyphosphazenes and polysiloxanes, and good chemical stability similar to that of the polyolefins [1–8]. It was found that the Si–C backbone of these polymers provided thermal stability similar to, or even better than, that of polysiloxanes [9]. The Si–C backbone offers the prospect of improved backbone hydrolytic stability over the polysiloxanes, particularly under strongly basic conditions [8]. The crystal structures of the PSMs have not been reported except for the unsubstituted polymer polysilaethylene (PSE) [10]. A more extensive study of poly(*n*-propylsilylenemethylene) (PDPrSM) has been reported separately [11].

PSE was found to adopt a planar zigzag conformation in the solid state, packing in a unit cell having dimensions $a = 5.70$ Å, $b = 8.75$ Å, c(fiber axis) $= 3.25$ Å and $\gamma = 97.6°$ [10]. PDPrSM, on the other hand, is triclinic with unit cell parameters $a = 10.52$ Å, $b = 8.66$ Å, $c = 4.86$ Å, $\alpha = 78.4°$, $\beta = 100.0°$ and $\gamma = 98.2°$ [11]. Its fiber repeat indicates an all-*gauche* conformation in the main chain, giving a 4_1 helical structure. Semi-empirical energy calculations show that polymers having *n*-alkyl side chains attached to the main chain have their lowest energy in an all-*gauche* conformation, while the unsubstituted polymer, PSE, has its minimum energy at an all-*trans* conformation [11,12]. The change from the all-*trans* backbone conformation of PSE to the all-*gauche* conformation of PDPrSM arises from intramolecular steric crowding near the backbone.

In this paper, we report results from X-ray and electron diffraction (ED) on the structures of other PSMs having *n*-alkyl side chains ranging from ethyl to hexyl. The results provide further insight into the influence of the side chains on the backbone conformation and chain packing.

2. Experiment

Fiber specimens for X-ray work were prepared by drawing isotropic melts on a glass slide at 80°C with tweezers. Wide angle X-ray patterns were recorded on both Kodak Direct Exposure film and a phosphor image plate

---

[*] Corresponding author. Air Force Research Laboratory, Materials and Manufacturing Directorate, 2941 P St. Suite 1, Wright–Patterson Air Force Base, OH 45433-7750, USA. Tel.: +1-937-255-9209; fax: +1-937-255-9157.

E-mail address: barry.farmer@afrl.af.mil (B.L. Farmer).

0032-3861/01/$ - see front matter © 2001 Published by Elsevier Science Ltd.
PII: S0032-3861(00)00772-2

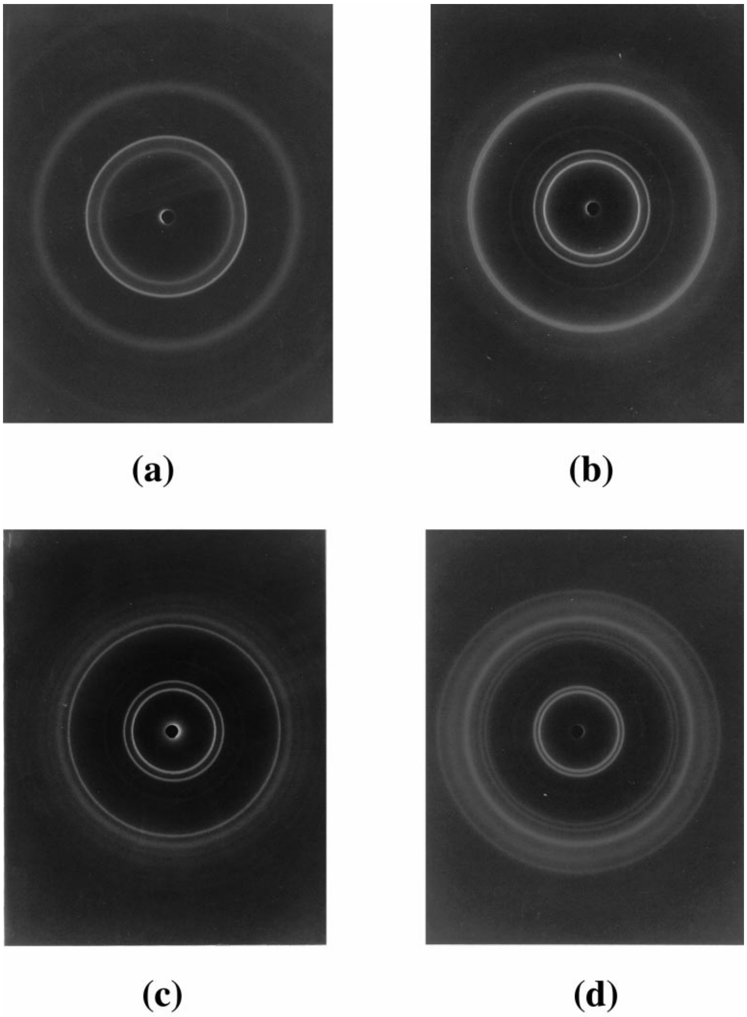

Fig. 1. Powder X-ray patterns of: (a) PDESM; (b) PDBSM; (c) PDPeSM; and (d) PDHSM.

Table 1
The observed (d_o) and calculated (d_c) *d*-spacings of *hk*0 reflections of PDESM from electron and X-ray diffraction based on a two dimensional reciprocal unit cell with dimensions $a^* = 1/13.58$ Å^{-1}, $b^* = 1/9.04$ Å^{-1} and $\gamma^* = 87.6°$

h	*k*	*l*	d_o(ED), Å	d_c, Å	d_o(X-ray), Å	I
2	0	0	6.79	6.79	6.78	VS
4	0	0	3.38	3.38	3.39	M
−1	1	0	7.66	7.67	8.05	S
−3	1	0	4.07	4.12	3.86	W
0	2	0	4.52	4.52	4.51	W
0	3	0	3.02	3.01		W
					4.32	M
					3.42	W
					3.18	W
					2.92	W
					2.59	W
					2.49	w

(Molecular Dynamics©) in a Statton camera using monochromated CuKα radiation from a Rigaku rotating anode X-ray generator operated at 50 KV and 150 mA. The sample to film distance was calibrated by SiO_2 powders.

Samples suitable for transmission electron microscopy (TEM) and ED were prepared by casting thin films on carbon-coated glass cover slides. A drop of 0.05 wt% solution of polymer in toluene was evaporated, melted and crystallized at the desired temperature in a Mettler hot stage. The sample was shadowed with Pt/C at ~15° incidence or by gold decoration at normal incidence, floated on water [with the help of poly(acrylic acid) as needed] and mounted on copper grids. ED patterns were obtained using a Philips CM-200 TEM with cooling stage in selected area mode under low-irradiation conditions. ED patterns were recorded on film immediately after observation because the sample was quickly damaged by the electron beam. The macroscopic structure of single crystals was observed through an optical microscope (Leitz Ortholux) using crossed polarizing filters.

Table 2
The observed (d_o) and calculated (d_c) d-spacings of $hk0$ reflections of PDBSM from electron and X-ray diffraction based on a two dimensional reciprocal unit cell with dimensions $a^* = 1/11.24$ Å^{-1}, $b^* = 1/9.40$ Å^{-1} and $\gamma^* = 80.5°$

h	k	l	d_o(ED), Å	d_c, Å	d_o(X-ray), Å	I
1	0	0	11.23	11.24	11.33	VS
2	0	0	5.63	5.62		W
3	0	0	3.75	3.75	3.78	M
−3	1	0	3.70	3.70		W
−2	1	0	5.22	5.22		W
−1	1	0	7.92	7.88	7.90	S
0	1	0	9.40	9.40	9.35	VS
1	1	0	6.65	6.69	6.72	S
2	1	0	4.51	4.51	4.53	VS
3	1	0	3.29	3.30	3.31	M
4	1	0	2.58	2.58		W
5	1	0	2.11	2.11		W
6	1	0	1.77	1.78		W
−3	2	0	3.21	3.20		W
−2	2	0	3.95	3.94	3.96	S
−1	2	0	4.63	4.62	4.62	VS
0	2	0	4.69	4.70		S
1	2	0	4.10	4.10		W
2	2	0	3.35	3.34		W
3	2	0	2.71	2.72		W
4	2	0	2.25	2.25		W
6	2	0	1.66	1.65		W
−3	3	0	2.62	2.63		VW
−2	3	0	2.96	2.95		VW
−1	3	0	3.16	3.16	3.16	M
0	3	0	3.13	3.13		W
1	3	0	2.90	2.90		W
2	3	0	2.56	2.56		W
3	3	0	2.23	2.23		VW
4	3	0	1.93	1.94		W
−3	4	0	2.15	2.16		W
−1	4	0	2.37	2.38		W
0	4	0	2.34	2.35		W
					4.52	M
					3.06	W
					2.83	W
					2.52	W
					2.41	W
					2.55	W
					2.32	W
					2.12	W

Table 3
The observed (d_o) and calculated (d_c) d-spacings of $hk0$ reflections of PDPeSM from electron and X-ray diffraction based on a two dimensional reciprocal unit cell with dimensions $a^* = 1/12.49$ Å^{-1}, $b^* = 1/10.46$ Å^{-1} and $\gamma^* = 82.2°$

h	k	l	d_o(ED), Å	d_c, Å	d_o(X-ray), Å	I
1	0	0	12.49	12.49	12.36	VS
2	0	0	6.28	6.25	6.22	W
2	1	0	5.09	5.07	5.04	W
1	1	0	7.60	7.53	7.48	S
0	1	0	10.46	10.46	10.43	VS
−1	1	0	8.72	8.62	8.59	S
0	2	0	5.27	5.23	5.25	W
−1	2	0	5.14	5.08	5.04	W
					4.66	M
					4.31	W
					4.16	W
					4.07	W
					3.68	W
					3.48	W
					3.23	W
					3.01	W
					2.32	W
					2.12	W

Table 4
The observed (d_o) and calculated (d_c) d-spacings of $hk0$ reflections of PDHSM from electron and X-ray diffraction based on a two dimensional reciprocal unit cell with dimensions $a^* = 1/12.83$ Å^{-1}, $b^* = 1/11.74$ Å^{-1} and $\gamma^* = 81.7°$

h	k	l	d_o(ED), Å	d_c, Å	d_o(X-ray), Å	I
1	0	0	12.83	12.83	12.98	VS
2	0	0	6.41	6.42	6.47	W
3	0	0	4.28	4.28	4.25	W
−1	1	0	9.36	9.36	9.35	W
0	1	0	11.74	11.74	11.64	VS
1	1	0	8.09	8.10	8.04	W
2	1	0	5.31	5.32	5.34	S
3	1	0	3.84	3.84	3.89*	S
−2	2	0	4.65	4.68	–	W
−1	2	0	5.67	5.66	5.66	S
0	2	0	5.87	5.87	5.88	S
1	2	0	5.06	5.07	5.05	W
−1	3	0	3.90	3.90	3.89*	S
0	3	0	3.93	3.91	3.89*	W
					4.74	M
					3.58	W
					3.45	W
					3.30	W
					3.20	W
					2.91	W
					2.72	W
					2.60	W
					2.49	W
					2.42	W
					2.31	W
					2.13	W
					2.08	W
					1.99	W

* Overlapping reflections.

3. Results and Discussion

Fig. 1 shows the powder X-ray diffraction patterns of PDESM, PDBSM, PDPeSM and PDHSM. The observed d-spacings are listed in Tables 1–4. The first and second Bragg reflections are very strong in all powder patterns. Fig. 2 shows a plot of the observed d-spacings of the first, second and third reflections plotted against the number of methylene units in the n-alkyl side chains. Values for PDPrSM are taken from Ref. [11]. There is linear relationship except for the shortest side chain material, PDESM. These three reflections were indexed as 100, 010 and −110 (except for those of PDESM). These indices were confirmed by ED (which will be discussed later). The

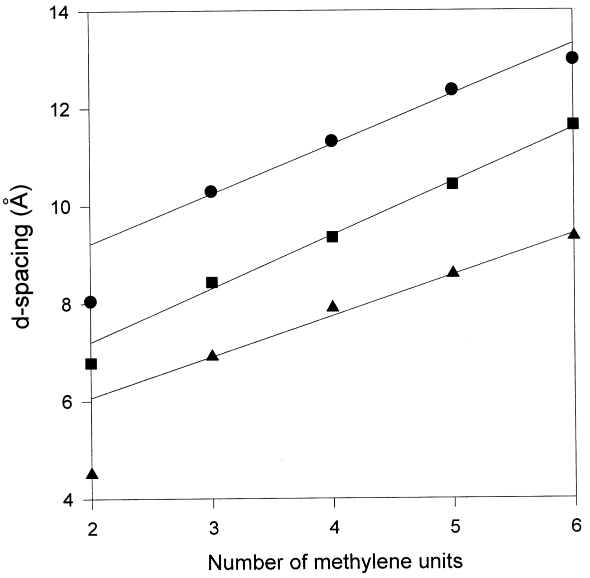

Fig. 2. *D*-spacings of the first, second and third Bragg reflections *versus* the number of methylene units in the alkyl side chain (●: first Bragg reflection, ■: second Bragg reflection, ▲: third Bragg reflection).

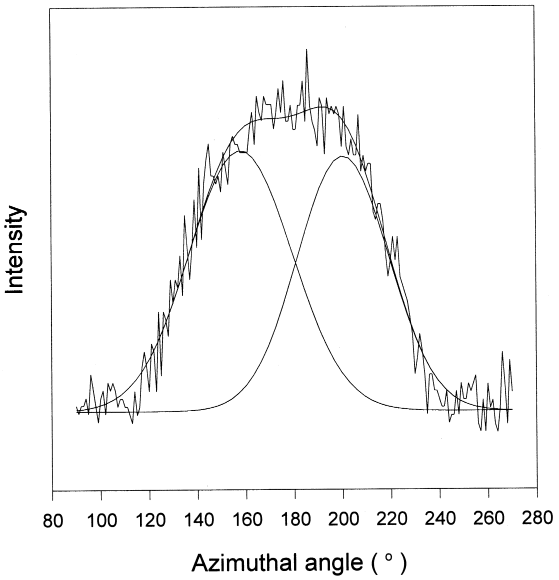

Fig. 4. Azimuthal scan of the reflection at $d = 4.32$ Å and its resolution into two maxima.

d-spacings of the 100, 010 and −110 reflections represent the dimensions related to the *ab*-projection of the unit cell (the fiber axis is taken as *c*). Thus, the cell dimensions of the *ab*-projection increase in proportion to the length of the side chain while the basic shape of the *ab*-projection of the unit cell remains the same. This linear relationship strongly suggests that the chains are packed in similar fashion in the unit cells and that the backbone conformations are the same. (A change of the backbone conformation usually brings a different cross-sectional shape to the polymer molecule and therefore different packing and shape of the *ab*-projection of the unit cell). The slopes of the lines are 0.9, 1.1 and 0.8 Å per methylene unit for the 100, 010, and −110 reflections, respectively. These slopes are smaller than that of the most extended case (~1.25 Å/methylene) suggesting either that the side chains do not extend in directions normal to these planes, that the side chains are not in a planar zigzag conformation, or both. A detailed study of the side chain conformation is in progress.

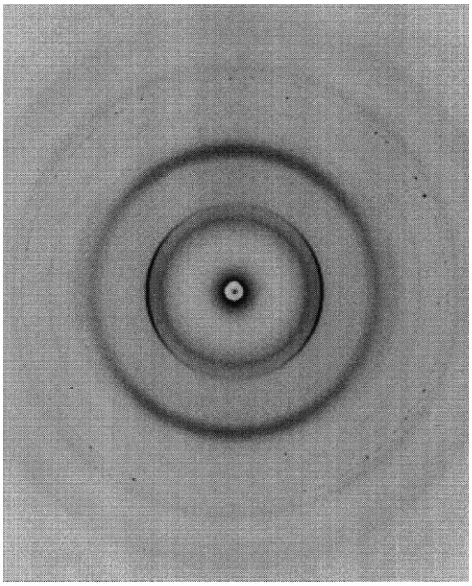

Fig. 3. The fiber X-ray pattern of PDESM (vertical direction is fiber direction).

The deviation of PDESM from the line indicates that PDESM packs differently from the other PSMs. Fig. 3 shows an X-ray pattern from a sample of PDESM having a small degree of orientation. Close examination allows the *l* index of some of the reflections to be discerned. The first and second Bragg peaks of Fig. 3 are located on the equator at $d = 8.05$ and 6.78 Å, indicating that these are *hk*0 reflections. The *d*-spacing of the first reflection on the first layer line is 4.32 Å, indicating that the fiber repeat is larger than 4.32 Å. An all-*trans* conformation of the backbone gives a fiber repeat of 3.17 Å. Thus the backbone conformation of PDESM is not all-*trans*. This is in contrast to PSE, which does have an all-*trans* conformation [10].

The peak at $d = 4.32$ Å can actually be separated into two peaks, as shown in Fig. 4. The azimuthal angle of maximum intensity of the separated peaks is 23° from the meridian (180°). From this position, the calculated fiber repeat (after correction for curvature of the layer line) is ~4.8 Å, very close to the fiber repeat expected from an all-*gauche* conformation (~4.86 Å). The conformational energy of PDESM is also reasonable for an all-*gauche* conformation [11]. Further, the backbone conformation of PDPrSM is known to be all-gauche [11].

PSMs having side chains other than ethylene and propylene were difficult to draw into fibers. Optical microscopy, electron microscopy and ED methods were employed to

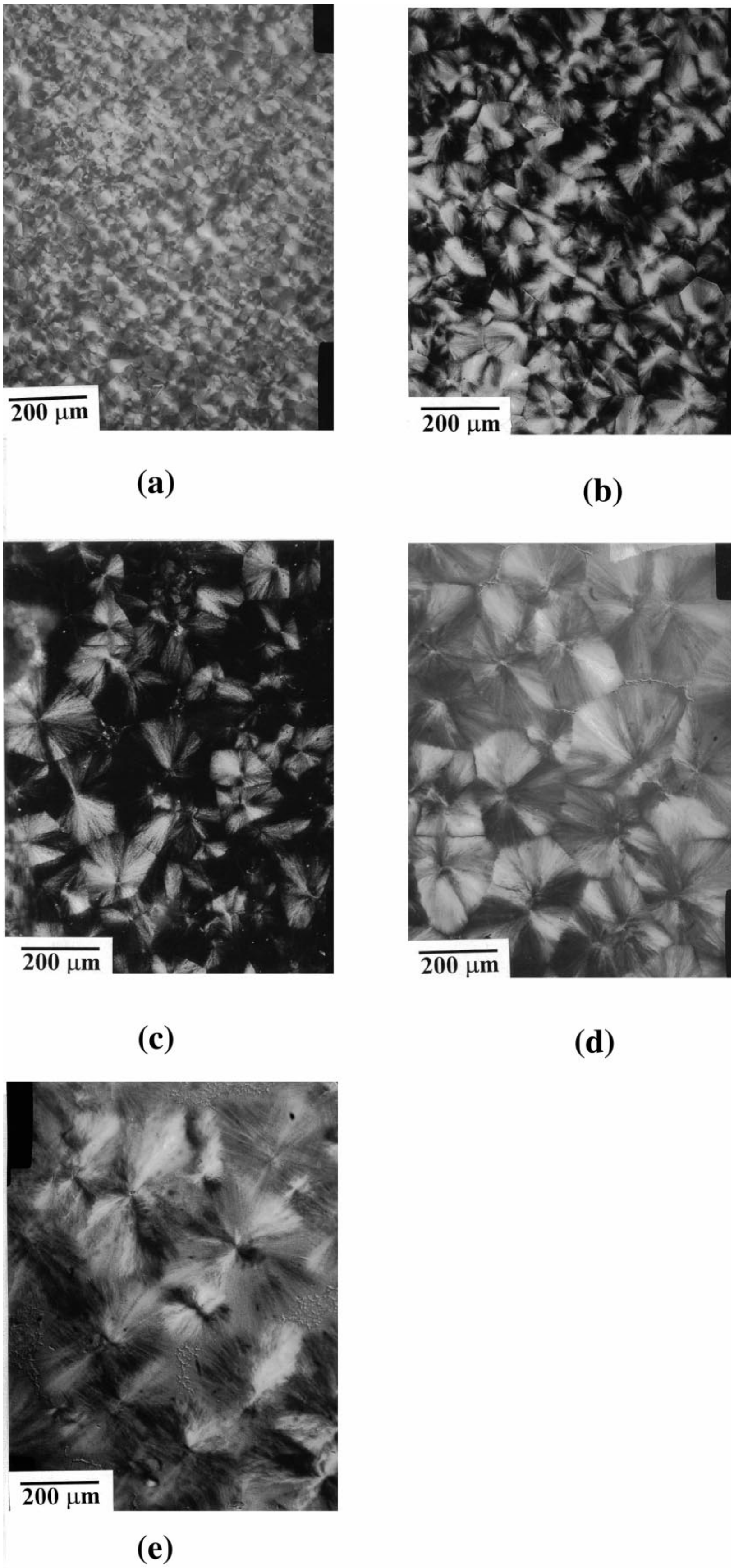

Fig. 5. Optical micrographs of spherulites of PDHSM grown between cover slides at: (a) 40°C; (b) 45°C; (c) 50°C; (d) 53°C; and (d) 58°C. (Crossed polarizing filters were used.)

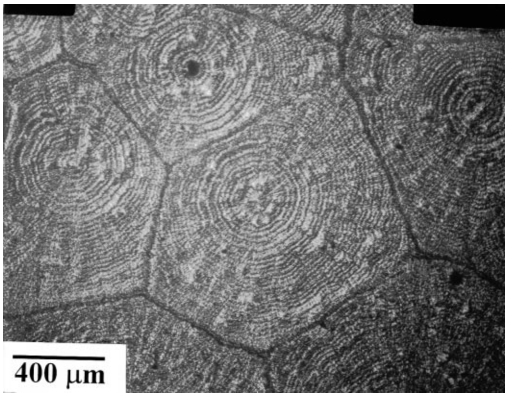

Fig. 6. Optical micrographs of the banded structure of PDHSM spherulites grown at ~50°C without the cover glass.

analyze the structure of these PSMs. Fig. 5 shows the spherulites of PDHSM grown between cover slides at 40, 45, 53 and 58°C. The spherulites grown at 58°C are almost 0.5 mm in diameter. A radiating structure and Maltese cross are observed. Similar spherulites were observed for the other PSMs. The banded structure shown in Fig. 6 was seen in PDHSM grown at ~50°C without a cover glass. This banded structure indicates that the radiating units are twisted about their axes [13]. The period of the twisting corresponds to the spacing of the rings which is ~20 μm.

Fig. 7 shows optical micrographs of dendrites of PDESM, PDBSM and PDHSM which were grown from thin films at ~55°C. Similar dendritic structures having secondary and tertiary branching were observed for all the materials except for PDESM. Fig. 8 shows the TEM picture of the lamella of PDHSM. The rectangular lamellae are ~0.5 μm wide.

Fig. 9 shows the ED patterns of PDESM, PDBSM,

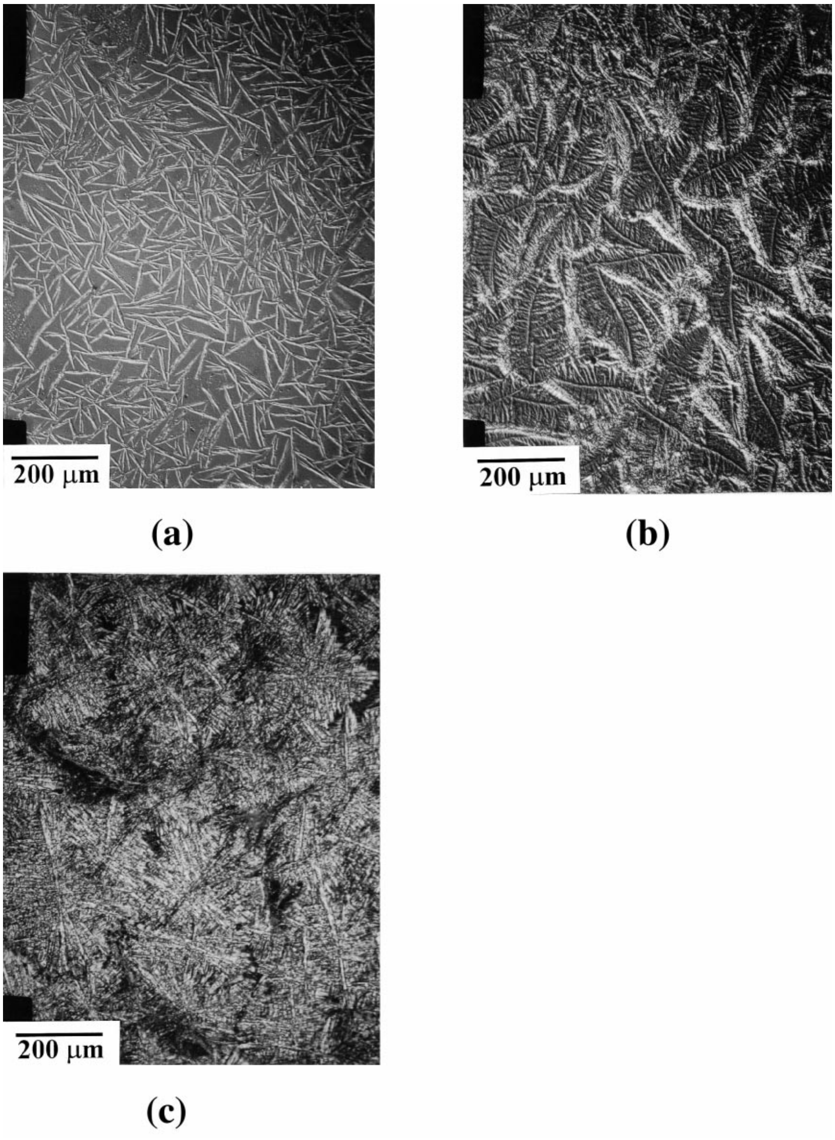

Fig. 7. Optical micrographs of hedrites of: (a)PDESM; (b) PDBSM; and (c)PDHSM grown at 55°C from thin films.

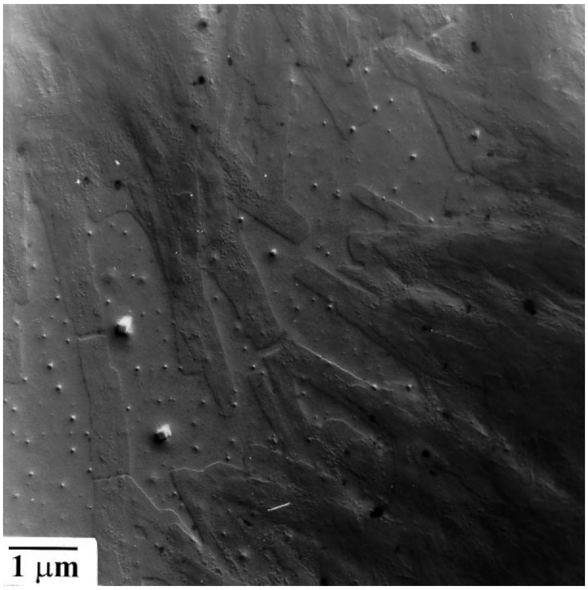

Fig. 8. TEM picture of lamellae of PDHSM.

PDPeSM and PDHSM taken with the electron beam perpendicular to the film surface. The observed reflections were *hk*0 reflections as listed in Tables 1–4. The observed *d*-spacings from X-ray and ED agree well with each other. The ED patterns of all the PSMs (except that of PDESM) are similar, each showing monoclinic symmetry.

As expected from the X-ray data, the ED pattern (Fig. 9a) of PDESM has nearly orthorhombic symmetry. The two sharp reflections in the horizontal direction at $d = 6.8$ and 3.4 Å can be indexed as 200 and 400. Similarly the two sharp reflections in near-vertical direction at $d = 4.5$ and 3.0 Å can be indexed as 020 and 030. Thus d_{100} and d_{010} are 13.6 and 9.0 Å, respectively. The angle between a^* and b^* (γ^*) is 88° suggesting a nearly orthorhombic structure. The larger unit cell of PDESM (compared to that of the other PSMs, see below) indicates that there is more than one chain in the unit cell. The calculated density is 1.106 g cm^{-3} with two chains (four monomer units each) in the unit cell assuming the fiber repeat is all-*gauche* ($c = 4.86$ Å). The absence of 100 and 010 reflections also strongly suggests that there is a second chain in the unit cell, possibly positioned in the middle of the *ab*-projection of the unit cell. However, the appearance of a very weak 030 reflection indicates that there is not perfect *C*-centered symmetry. The second chain may therefore have a different setting angle in the unit cell, or may be slightly shifted off-center.

The diffraction pattern of PDHSM (Fig. 9d), is composed of two sets of diffraction spots from structures related by a mirror plane perpendicular to a^*; i.e. a twin structure. The

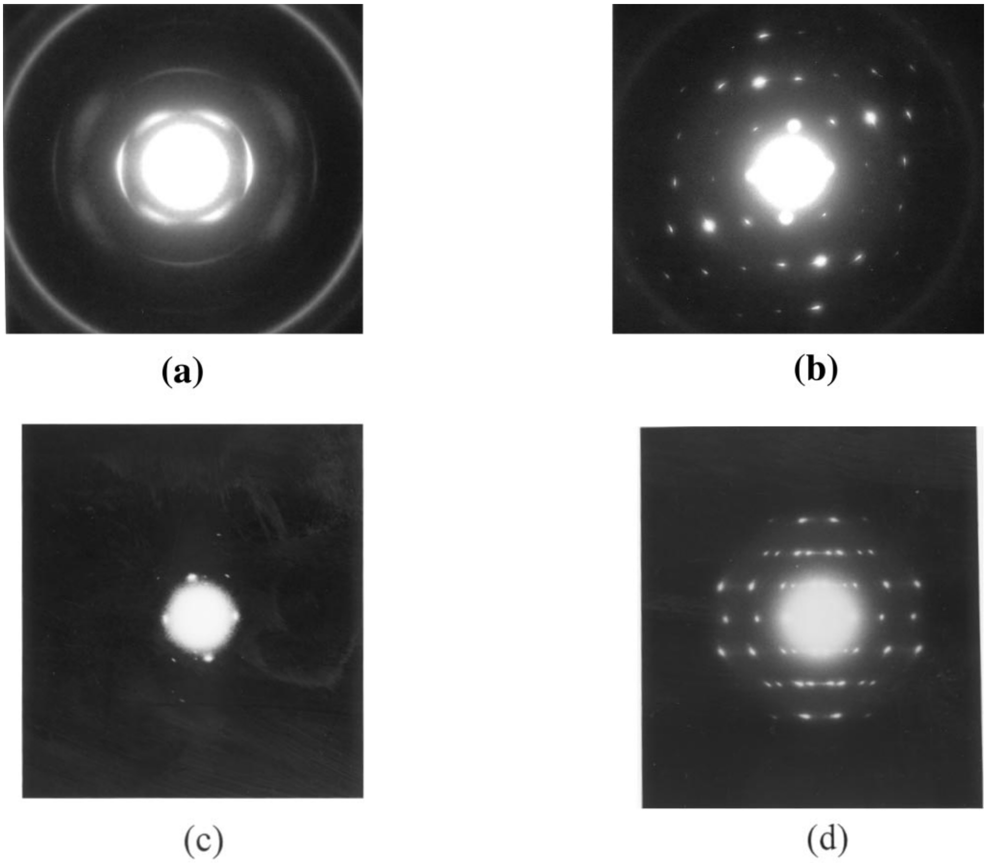

Fig. 9. The ED patterns of: (a) PDESM; (b) PDBSM; (c) PDPeSM; and (d) PDHSM. The electron beam was perpendicular to the film. (a^* is horizontal and b^* is nearly vertical).

Table 5
Two dimensional unit cell dimensions, the number of monomer units in the unit cell (*N*) and calculated densities (ρ_c) of PSMs assuming a fiber repeat of 4.86 Å (all-*gauche* conformation)

	$d_{100}(1/a^*)$, Å	$d_{010}(1/b^*)$, Å	$\gamma^*(°)$	N	$\rho_c(\mathrm{g\ cm^{-3}})$
PDESM	13.58	9.04	87.6	4	1.106
PDPrSM [11]	10.30	8.42	83.6	2	0.995
PDBSM	11.24	9.40	80.5	2	0.982
PDPeSM	12.49	10.46	82.2	2	0.948
PDHSM	12.83	11.74	81.7	2	0.946

d-spacing of the first strong diffraction spot in the horizontal direction is 12.98 Å, the same as the first Bragg reflection in the X-ray powder pattern. Similarly the *d*-spacing of the first strong spot in the near-vertical direction is 11.64 Å, the same as the second Bragg reflection in the X-ray powder pattern. These two reflections can be indexed as 100 and 010. The γ^* angle between 100 and 010 is 82.8°. Similar a^*, b^* and γ^* values for PDESM, PDPrSM [11], PDBSM and PDPeSM were determined as listed in Table 5. The calculated densities (assuming an all-*gauche* conformation with $c = 4.86$ Å and one chain per cell) were 0.98 ± 0.03 g cm^{-3} which is typical of those measured for other silicon–carbon polymers such as poly(di-*n*-alkylsilanes) [14].

An interesting aspect of the diffraction patterns shown in Fig. 9 is the intensity distribution of the *hk*0 reflections. For example, the ED patterns of all PSMs have relatively strong −120, and 210 reflections, suggesting that the side chains may be oriented in these reflection planes. This is consistent with the slopes of d_{100} and d_{010} versus the number of side chain methylene units shown in Fig. 2. A detailed study of chain packing of PSMs using energy calculations is in progress.

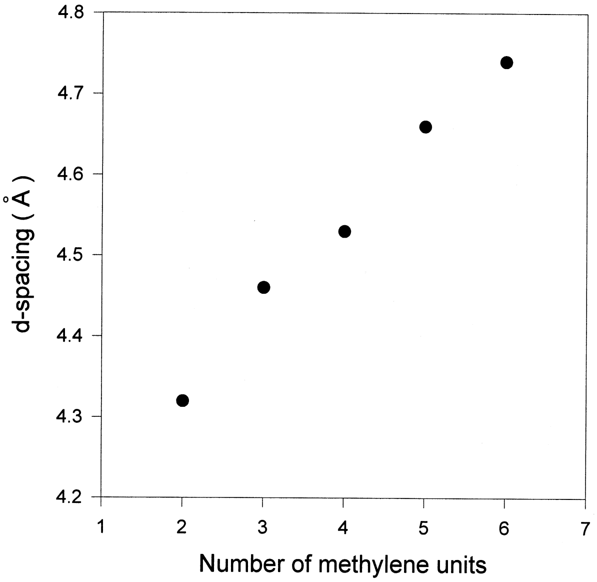

Fig. 10. Plot of *d*-spacing for the first non-*hk*0 Bragg peak *versus* number of methylene units in the side chain.

Fig. 10 shows the *d*-spacing of the first Bragg peak in the X-ray patterns which was not an *hk*0 reflection for each of the PSMs (these peaks are not seen in the *hk*0 ED patterns). These peaks are relatively strong at ~4.5 ± 0.3 Å in the powder X-ray patterns of Fig. 1. One characteristic of these reflections is that they are broad compared to the sharp *hk*0 reflections. For PDESM and PDPrSM (from which fiber patterns could be obtained), these peaks are located on the first layer line [11]. It is reasonable to assume, therefore, that the corresponding reflections from PDBSM, PDPeSM and PDHSM are also *hk*1 reflections. The *d*-spacings increase linearly as the side chain length increases. The increasing *d*-spacing can be attributed to dilation of *a* and *b* dimensions while the fiber repeat (*c*) remains unchanged. All the reflections have *d*-spacings in the range of 4.3–4.8 Å. The backbone conformation, therefore, cannot be all-*trans* because the fiber repeat must be at least as large as these values (all-*trans* repeat is 3.17 Å). The most likely conformation is all-*gauche* which gives a fiber repeat ~4.86 Å. This all-*gauche* conformation is observed experimentally for PDESM and PDPrSM and is calculated to be energetically feasible [11].

4. Conclusions

The structures of PDESM, PDBSM, PDPeSM and PDHSM have been studied using X-ray and ED methods. The *d*-spacings of the 100, 010 and −110 reflections of PDPrSM [11], PDBSM, PDPeSM and PDHSM in the powder X-ray patterns increase linearly with side chain length, indicating that PDPrSM, PDBSM, PDPeSM and PDHSM have similar packing and all have one chain in the unit cell. PDESM deviates from the linear relationship between *d*-spacing and alkyl side chain length shown by the other polymers. It has nearly orthorhombic symmetry ($\gamma^* = \sim 88°$) in the *hk*0 ED pattern. The unit cell contains two chains (with four repeat units each) in contrast to the other PSMs. The absence of 100 and 010 reflections in the ED pattern of PDESM suggests that the second chain is located near the center of the *ab*-projection of the unit cell.

The fiber X-ray patterns of PDESM and PDPrSM show that the backbone conformations are all-*gauche,* giving a 4_1 helical structure. Taken together, the results from X-ray and ED show that the backbone conformations of the other PSMs such as PDBSM, PDPeSM and PDHSM are also all-*gauche*. Contrasting PDESM with the other PSMs studied, the results indicate that the length of the side chains can affect the chain packing in the unit cell without changing the backbone conformation.

Acknowledgements

We thank Prof. P. Geil for the useful advice and discussion about growing single crystals. Support from National

Science Foundation through grant DMR-9731345 is gratefully acknowledged.

References

[1] Laine RM, Babonneau F. Chem Mater 1993;5:260.
[2] Seyferth D, Lang H. Organometallics 1991;10:551.
[3] Birot M, Dunogues J-P. J Chem Rev 1995;95:1443.
[4] Mark JE, Allcock HR, West R. Inorganic polymers. New York: Prentice Hall, 1992. p. 154.
[5] Bazant V, Chvalovsky V, Rathousky J. Organosilicon compounds. New York: Academic Press, 1965. p. 47.
[6] Bacque E, Pillot J-P, Birot M, Dunoges J. Macromolecules 1988;21:30.
[7] Habel W, Mayer L, Sartory P. J Organomet Chem 1994;474:63.
[8] Rushkin IL, Interrante LV. Macromolecules 1996;29:3123.
[9] Levin G, Carmichael JB. J Polym Sci, A-1 1968;6:1.
[10] Tsao M-W, Pfeifer K-H, Rabolt JF, Holt DB, Farmer BL, Interrante LV, Shen Q. Macromolecules 1996;29:7130.
[11] Park SY, Interrante LV, Farmer BL. Polymer 2000.
[12] Interrante LV, Wu H-J, Apple T, Shen Q, Zeimann B, Narsavage DM. J Am Chem Soc 1994;116:12,085.
[13] Geil PH. Polymer single crystals. New York: Wiley, 1973 (chap. 4).
[14] KariKari EK, Greso AJ, Farmer BL, Miller RD, Rabolt JF. Macromolecules 1993;26:3937.